Int. J. Heat Mass Transfer. Vol. 36, No. 6, pp. 1477–1484, 1993
Printed in Great Britain

0017-9310/93 $6.00 + 0.00

Mixed convection in a suddenly-expanded channel with effects of cold fluid injection

C. Y. SOONG
Department of Aeronautical Engineering, Chung Cheng Institute of Technology, Taoyuan, Taiwan 33509, R.O.C.

and

W. C. HSUEH
Department of System Engineering, Chung Cheng Institute of Technology, Taoyuan, Taiwan 33509, R.O.C.

(*Received* 7 *January* 1992 *and in final form* 21 *July* 1992)

Abstract—This paper deals with a numerical study on mixed convection in a horizontal suddenly-expanded channel with a cold fluid injected along the backward-facing wall. Navier-Stokes/Boussinesq equations are solved by using the SIMPLER algorithm on a non-uniform staggered grid system. Effects of the foreign fluid injection and free convection on the flow and heat transfer characteristics are examined. For small amounts of cold fluid injection, the results reveal noticeable enhancement in local heat transfer rate on the backward-facing wall but slight degradation on the bottom wall beneath the separation bubble. The recirculation zone can be enlarged by either the foreign fluid injection and buoyancy force, and the physical interpretation about these mechanisms are addressed. Bi-linear correlations are proposed for the predictions of reattachment length at various injection and buoyancy conditions.

INTRODUCTION

FLOW FIELDS with recirculation zones have long been an interesting subject due to the relevance to a variety of engineering problems such as the flows over blunt-based vehicles, flame-holders, dump combustors, chips mounted on PC-board in electronic equipment, etc. In the presence of the flow separation and re-attachment, the flow structure and the associated convective heat transfer become complicated. Various separated flow configurations were investigated in previous studies, while the backward-facing step flow may be the most typical one on which the focused attention has been concentrated. In the past decades, numerous studies were reported on this class of flows. Most of the published work related to the hydrodynamic characteristics [1–8], and if heat transfer, e.g. [9, 10], pure forced convection was concerned with. Only a few recent works were related to combined free and forced convection in the separated flows. Chou and Wu [11] studied mixed convection in a horizontal channel with a surface mounted block. In a partially blocked vertical channel, the mixed convection has been studied by Habchi and Acharya [12]. Most recently, Lin *et al.* [13] reported a numerical study on the buoyancy-assisting effects on flow and heat transfer in the vertical backward-facing step flows. Their results showed that the free-convection significantly affects the reattachment process and, therefore, the convective transport in this class of separated flows.

Foreign fluid injection is an effective means for flow and thermal controls. In thermal systems, a cold fluid can be introduced into devices for cooling of hot elements. Since the flow in a recirculation zone is diffusion-dominated, the heat convection in the region is relatively low. A cold fluid injection may be used to improve heat transfer performance in separated flows. The effects of bottom injection on flow and heat transfer in rectangular cavities have been reported in a recent study [14], in which the hot fluid injection was considered and the free-convection effect was ignored.

In the present investigation a different situation is dealt with. The step and the bottom walls are considered as heat sources and, for cooling of the system, an injected cold fluid is used as coolant. To retain a better understanding of this complex flow, the mixed convection in a horizontal suddenly-expanded channel with a cold fluid injection from the step root corner and along the backward-facing wall is considered. The improvement of local heat transfer on the backward-facing wall can be expected; however, the influences of the injection and buoyancy on the convective transport in the recirculation zone are not so trivial and are well worth investigating.

ANALYSIS

Governing equations

Figure 1 shows schematically the flow configuration considered in the present study, which is a two-dimensional channel with an asymmetric sudden-expansion. The channel height is D, the step height is S, and,

NOMENCLATURE

D, d	dimensional and dimensionless channel height, $d = D/S$
E	expansion ratio, $D/(D-S)$
g	gravitational acceleration
Gr	Grashof number, $g\beta(T_w - T_o)S^3/\nu^2$
h	heat transfer coefficient
k	thermal conductivity
L, l	dimensional and dimensionless length, $l = L/S$
Nu	Nusselt number, hs/k
P	static pressure
P', p'	dimensional and dimensionless pressure departure, $p' = P'/\rho\bar{U}_o^2$
Pe	Peclet number, $Pr\,Re$
Pr	Prandtl number, ν/α
Re	main flow Reynolds number, $\bar{U}_o S/\nu$
Ri	Richardson number, Gr/Re^2
S	step height
T	temperature
$\bar{U}$	mean velocity
U, V	dimensionless velocity components
u, v	dimensional velocity components
X, Y	Cartesian coordinates
x, y	dimensionless coordinates, $(X, Y)/S$.

Greek symbols

α	thermal diffusivity
β	thermal expansion coefficient
θ	dimensionless temperature difference, $(T-T_o)/(T_w-T_o)$
μ	viscosity
ν	kinematic viscosity
ρ	density.

Subscripts

o	inlet
1	pre-expansion
2	post-expansion
j	injection
r	reattachment
w	wall.

therefore, the channel inlet height is $D-S$. In this nomenclature the parameter $E = D/(D-S)$, denoting the ratio of post- to pre-expansion heights, is defined as a channel-expansion parameter. The origin O of a Cartesian coordinate lies at the step root corner. The channel has a pre-expansion length L_1 and a post-expansion length L_2 as the upstream and downstream parts of the abrupt enlargement, respectively. An injection port of width L_j adjacent to the backward-facing wall is located at the step root corner, from where the coolant air is injected and forms a wall jet along the backward-facing wall. The main flow entering the channel is assumed to be fully-developed. The flow is assumed to be steady, laminar, and of constant physical properties. By invoking Boussinesq approximation, the buoyancy effect is accounted for and a linear relation, $\rho = \rho_o[-\beta(T-T_o)]$, is used to approximate the density variation in the body force term. The subscript o denotes the inlet condition, which is defined as a reference state. The dimensionless form of the governing equations can be expressed as follows:

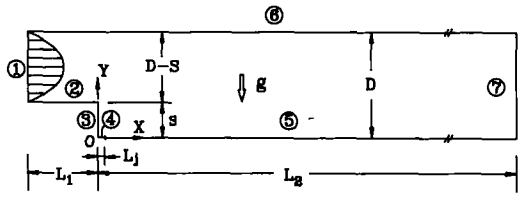

FIG. 1. Flow model and computational domain (Numbers in the circles correspond to the boundary conditions listed in the text).

$$\frac{\partial u}{\partial x} + \frac{\partial v}{\partial y} = 0 \tag{1}$$

$$u\frac{\partial u}{\partial x} + v\frac{\partial u}{\partial y} = \frac{1}{Re}\left(\frac{\partial^2 u}{\partial x^2} + \frac{\partial^2 u}{\partial y^2}\right) - \frac{\partial p'}{\partial x} \tag{2}$$

$$u\frac{\partial v}{\partial x} + v\frac{\partial v}{\partial y} = \frac{1}{Re}\left(\frac{\partial^2 v}{\partial x^2} + \frac{\partial^2 v}{\partial y^2}\right) - \frac{\partial p'}{\partial y} + \frac{Gr}{Re^2}\theta \tag{3}$$

$$u\frac{\partial \theta}{\partial x} + v\frac{\partial \theta}{\partial y} = \frac{1}{Pe}\left(\frac{\partial^2 \theta}{\partial x^2} + \frac{\partial^2 \theta}{\partial y^2}\right) \tag{4}$$

where

$$u = U/\bar{U}_o, \quad v = V/\bar{U}_o, \quad x = X/S, \quad y = Y/S,$$

$$p' = P'/\rho\bar{U}_o^2, \quad \theta = (T-T_o)/(T_w-T_o), \quad Re = \bar{U}_o S/\nu,$$

$$Pe = Pr\,Re, \quad Gr = g\beta(T_w-T_o)S^3/\nu^2.$$

In the above equations $\bar{U}_o$ and T_o denote average velocity and fluid temperature at the inlet; T_w stands for wall temperature, and Re, Pr, and Gr are the Reynolds, Prandtl, and Grashof number, respectively. For brevity, a combined parameter named Richardson number, $Ri \equiv Gr/Re^2$, is used to characterize the relative importance of buoyancy to forced convection.

Boundary conditions

To reduce the number of the parameters, some geometric parameters are specified. The size of the injection port and the pre-expansion lengths are specified as $l_j = L_j/S = 0.1$ or 0.2, and $l_1 = L_1/S = 2$, respectively. At the inlet plane, a parabolic velocity and a uniform fluid temperature are imposed. The upper wall of the channel is assumed to be adiabatic; but

the others, including the step and the bottom walls, remain isothermal. At the downstream boundary of the solution domain the axial gradients of the variables u, v and θ are assumed to vanish. To ensure the validity of this condition the post-expansion length has to be large enough. The magnitude of the post-expansion length is thus very critical. In ref. [15] Chein and Jwo studied the flow field in a channel with a rectangular heated block. In the case of block width/height ratio 5, channel-to-block ratio 4 and $Re = 1000$, they concluded that the fully-developed condition can be reached as long as the post-expansion length is larger than $9D$. For the backward-facing step flows at Reynolds numbers 60 to 230, Sparrow and Chuck [10] positioned the downstream boundary at $9D$, $12.33D$ and $13.75D$ for channels with $d = D/S = 2$, 3 and 4, respectively. Accordingly, the post-expansion length of $12.33D$ is a safety choice and is used through the present computations.

The boundary conditions on the boundaries numbered in Fig. 1 are summarized as follows:

(1) Channel inlet ($x = -2$, $1 \leqslant y \leqslant d$): $u-6\xi(1-\xi) = v = \theta = 0$ where $\xi = (y-1)/(d-1)$;
(2) Top surface of the step ($-2 < x < 0$, $y = 1$): $u = v = \theta - 1 = 0$;
(3) Backward-facing wall ($x = 0$, $0 < y < 1$): $u = v = \theta - 1 = 0$;
(4) Injection port ($0 < x < 0.2$, $y = 0$): $u = v - v_j = \theta = 0$;
(5) Bottom wall ($0.2 < x < 12.33d$, $y = 0$): $u = v = \theta - 1 = 0$;
(6) Upper wall ($-2 < x < 12.33d$, $y = d$): $u = v = \partial\theta/\partial y = 0$;
(7) Downstream open boundary ($x = 12.33d$, $0 \leqslant y \leqslant d$): $\partial u/\partial x = \partial v/\partial x = \partial\theta/\partial x = 0$.

NUMERICAL PROCEDURE

The system of the governing equations (1)–(4) are discretized by a control volume approach; and the convective terms are treated by the power-law scheme [16]. The resultant algebraic system is solved by line-by-line alternative direction implicit (ADI) method; and the SIMPLER algorithm [16] is employed for the treatment of pressure–velocity coupling. Before the main course of the computations, a numerical experiment was first carried out for grid-independence test. Results on 54×32, 64×48 and 80×54 grids were examined. The solutions on 64×48 and 80×54 grids agree well. To reduce the computational efforts, therefore, the 64×48 grid was chosen for the calculations through the entire study. The grid system is a non-uniform, staggered one and is clustered near the walls. For the injection port ($0 \leqslant x \leqslant 0.2$), five grid spaces in axial direction were arranged. Under-relaxation factors 0.7, 0.55, 0.7 and 0.9 were used in the iterative procedure for calculations of u, v, p, and θ, respectively. For high buoyancy cases, however, the smaller relaxation factors were employed. Stopping criteria were specified as the mass residuals being less than 10^{-4}. The computations were carried out on a VAX/8650 computer. In a typical computation 1500–2500 iterations (depending on initial guesses) were required to bring about convergence, which usually took 6–8 h of CPU time.

RESULTS AND DISCUSSION

Comparison with the previous studies

The results of the backward-facing step flows, especially the reattachment length, is sensitive to the numerical procedure used, and the boundary conditions including the inlet profiles, the location of the upstream boundary etc. For example, in a channel of specified expansion-ratio, different inlet velocity profiles may result in noticeable differences in the reattachment length. The adequateness of the present numerical procedure is evaluated by comparing the present predictions of reattachment location with that in the former literature.

In Fig. 2, for the channel with an expansion-ratio of $E = 1.5$, the numerical results by using the parabola [3–5, 8, 10] and a measured velocity profile [2–5] as the inlet condition, and the measurements [2] are plotted. The data scattering can be attributed to the slightly different boundary conditions and the numerical procedures in each studies. It is observed that the present results lie within the scattering band and agree reasonably well with the previous data.

Flow structure and temperature field

In the flow configuration considered, there are four major parameters involved, i.e. Reynolds number Re, expansion-ratio E, cold fluid injection velocity v_j, and buoyancy parameter Ri. Since the attention of the study is focused on the injection and free-convection effects, the numerical computations are carried out for the channel expansion-ratio $E = 1.5$ and the main flow Reynolds numbers $Re = 100$ and 50. Effects of

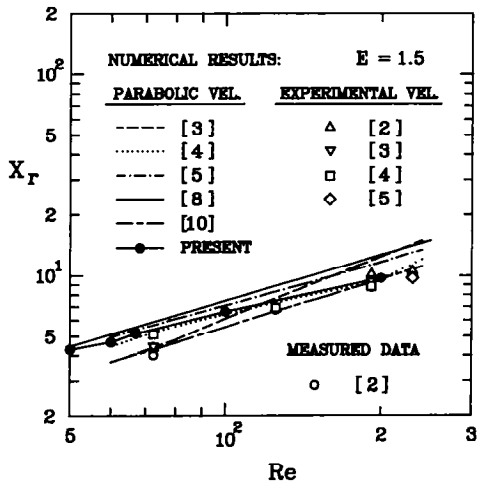

FIG. 2. Comparison of the reattachment length.

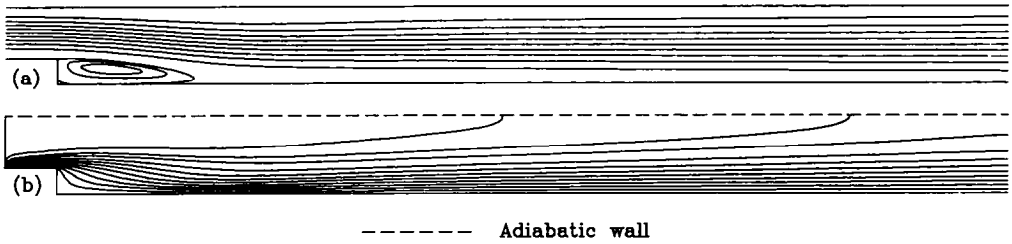

FIG. 3. Numerical results in entire flow field of (Re, E, v_j, Ri) = (100, 1.5, 0, 0): (a) streamline pattern; (b) isotherm contour.

the fluid injection are characterized by v_j which ranges from 0 to 0.2 in the present study. Consider, for example, chips of height 5–10 mm mounted on a PC board, the characteristic temperature difference $\Delta T_c = T_w - T_o = 30°C$ and the reference temperature $T_o = 300$ K, the buoyancy parameter Gr ranges from 500 to 3800. In the present study, therefore, Grashof numbers up to 4000 are studied.

Figure 3 shows the entire field solution of a baseline case: (Re, E, v_j, Ri) = (100, 1.5, 0, 0). As expected, a separation bubble lies behind the step and is enclosed by the dividing streamline, the bottom and the backward-facing walls. Also, in the isotherm contour, the isothermal lines locally perpendicular to the upper wall due to the adiabatic condition are presented. The flow and temperature fields seem likely to reach fully-developed conditions before arriving at the downstream boundary. To highlight the change of the flow field localized streamlines and isotherm contours will be presented hereafter.

The effects of fluid injection on the flow fields are shown in Fig. 4. Due to the displacement effect in wall shear layer the vertical wall-jet flow pushes the recirculation zone toward downstream. Meanwhile, due to the mass addition into the recirculation zone, the dividing streamline confining the recirculating flow have to be opened, and the injected fluid flows downstream between the dividing streamline and the circulatory flow. Since the main flow above the separated flow region is relatively strong, therefore, the bubble can more easily expand in the axial direction. This results in an elongation of the separation bubble. The effects of fluid injection on the temperature fields are revealed in Fig. 5. By comparing Fig. 5(a) with the subsequent contours 5(b)–(d), it is found that the noticeable changes in fluid temperature are presented

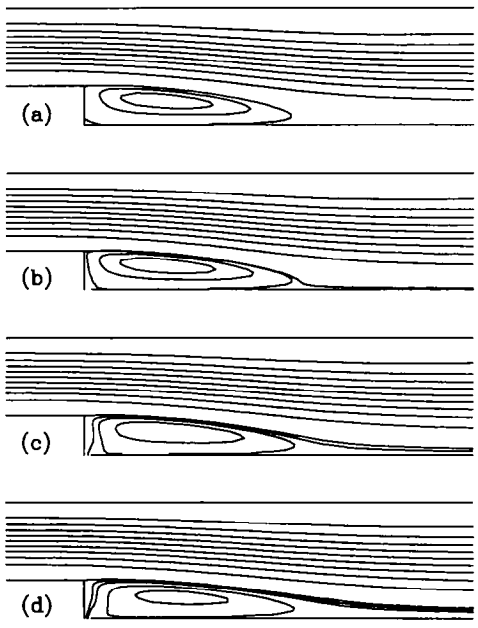

FIG. 4. Effects of foreign fluid injection on the flow structure for (Re, E, l_j, Ri) = (100, 1.5, 0.2, 0) and (a) $v_j = 0$; (b) $v_j = 0.01$; (c) $v_j = 0.1$, and (d) $v_j = 0.2$.

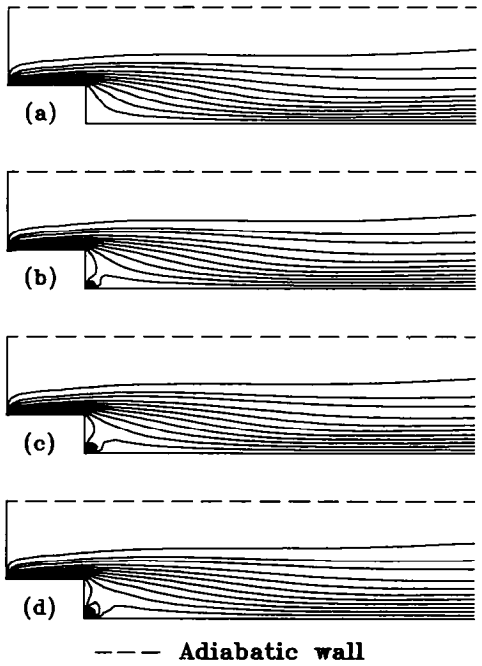

FIG. 5. Effects of foreign fluid injection on the temperature fields, (Re, E, l_j, Ri) = (100, 1.5, 0.2, 0) and (a) $v_j = 0$; (b) $v_j = 0.01$; (c) $v_j = 0.1$, and (d) $v_j = 0.2$.

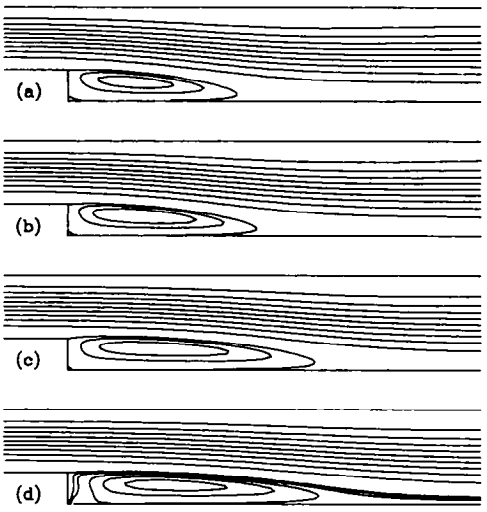

FIG. 6. Effects of free-convection on the flow structure, (Re, E, l_j) = (100, 1.5, 0.2) and (a) $v_j = Ri = 0$; (b) $v_j = 0$, $Ri = 0.1$; (c) $v_j = 0$, $Ri = 0.4$, and (d) $v_j = 0.2$, $Ri = 0.4$.

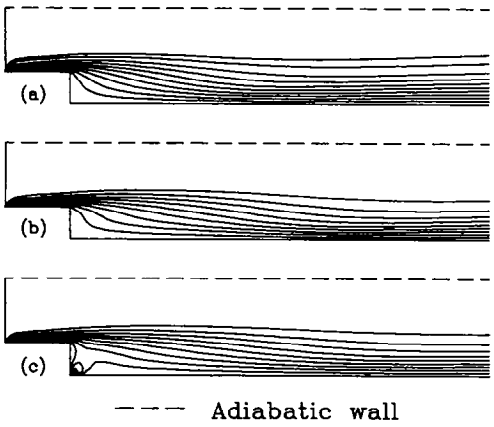

FIG. 7. Effects of free-convection on the temperature fields, (Re, E, l_j) = (100, 1.5, 0.2) and (a) $v_j = Ri = 0$; (b) $v_j = 0$, $Ri = 0.4$, and (c) $v_j = 0.2$, $Ri = 0.4$.

only in a region adjacent to the step and the injection port. Even a small injection velocity, $v_j = 0.01$ in Fig. 5(b), may cause an apparent modification in the isothermal contour.

The free-convection effects on the backward-facing step flows are presented in Fig. 6. In Figs. 6(a)–(c), the pure buoyancy effects are characterized by the buoyancy parameter $Ri = 0$, 0.1, 0.4. The size of the recirculation zone increases with the buoyancy. This can be attributed to the buoyancy-induced transverse motion near the bottom wall, which, in turn, displaces the streamlines upward and, therefore, widens as well as elongates the separation bubble. In the presence of the cold fluid injection, the coupled effect of buoyancy and injection is shown in Fig. 6(d). The combining effect results in the relatively longer bubbles. Figures 7(a)–(c) are the isotherm contours corresponding to the flows in Figs. 6(a,c,d). It is observed that the temperature field is not so sensitive to the buoyancy effect as the flow structure is.

Axial velocity profiles at a pre-expansion location, $x = -0.11$, and three post-expansion ones, $x = 0.15$, 3.73, and 6.75, are shown in Fig. 8. Apparently, the fluid injection has no significant effect on the velocity fields upstream. However, the downstream flow fields, especially that near the injection port, can be affected by the foreign fluid injection. The buoyancy effects on velocity fields are noticeable in the separation bubble and the further downstream parts; but are insignificant at the injection port and in pre-expansion region where the forced flow effects are strong.

Reattachment length

In Fig. 9(a) the influences of injection and buoyancy on the reattachment length are presented. Fortunately, the present predictions of the reattachment length are well correlated with the injection velocity and the buoyancy parameter in the parameter ranges considered. For the cases of $l_j = 0.2$, bi-linear correlations for x_r are proposed as

$$x_r = 6.6446 + 3.5701 v_j + 6.7160\, Ri; \quad \text{for} \quad Re = 100 \tag{5a}$$

and

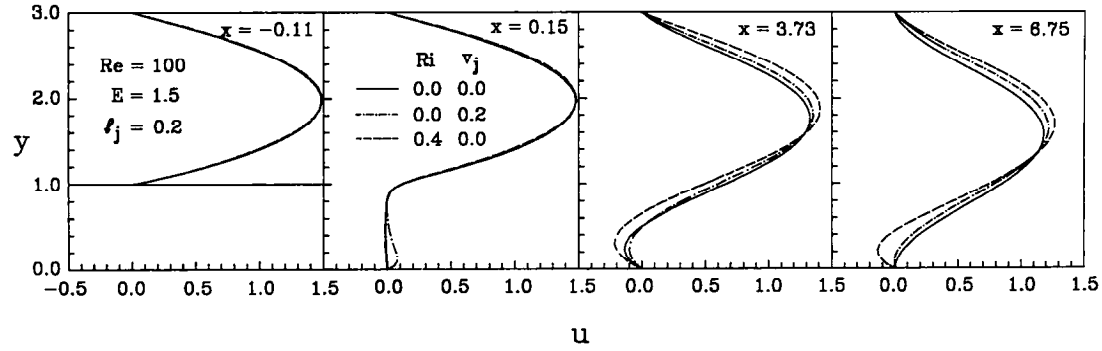

FIG. 8. Axial velocity distributions for (Re, E, l_j) = (100, 1.5, 0.2).

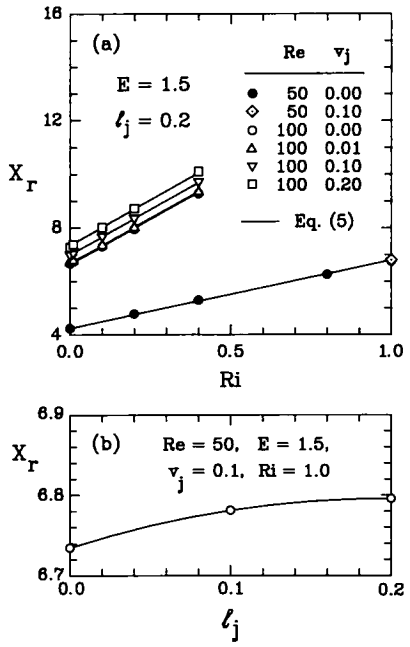

FIG. 9. Numerical predictions and correlations of reattachment lengths at various conditions: (a) effects of buoyancy and injection, and (b) effects of size of injection port.

$$x_r = 4.2525 + 0.4158 v_j + 2.5017\, Ri; \quad \text{for} \quad Re = 50. \tag{5b}$$

Equation (5) is accurate within 1.5%. In the present study only the injection port of small size, $0 \leqslant l_j \leqslant 0.2$, are studied. Figure 9(b) shows that the recirculation zone can be enlarged with increasing l_j but, in this l_j-range, the effects are small.

Local heat transfer rates

Local heat transfer rates on the top surface of the step, the backward-facing wall, and the bottom wall at various conditions are shown in Fig. 10. In Fig. 10(a), cold fluid injection provides no significant effects on heat transfer on the step top surface, but modifies that on the backward-facing and the bottom walls. Especially, the heat transfer enhancement near the lower part of the backward-facing wall is most striking. The results reveal that even at small injection velocity, $v_j = 0.01$, the improvement is remarkable; higher injection rates, $v_j = 0.1$ and 0.2, provide only relatively small beneficial effect. As for the heat transfer rates on the bottom wall, peak values of the Nusselt number occur near the reattachment points. The fluid injection moves the reattachment point downstream and therefore the location where the *Nu*-peak is located. The heat transfer on bottom wall beneath the separation bubble is alleviated with the increasing injection velocity.

Free-convection effects on heat transfer can be found in Fig. 10(b). The influences of buoyancy in the inlet region are negligibly small. The similar results for $Ri \leqslant 1.0$ were also disclosed in ref. [11]. It is noted that heat transfer enhancement by buoyancy, as that arising in usual mixed convection problem, is observed at the bottom wall downstream of the separation bubble. However, in the recirculation zone, i.e. on the backward-facing wall and the bottom wall covered by the bubble, the buoyancy degrades the heat transfer performance. It is believed that the buoyancy effect renders the circulatory fluid hotter, but the heated fluid cannot escape from the separation bubble. This phenomenon results in a heat transfer degradation in the recirculation zone; and a slightly upstream effect can be found on the top surface near the corner. For the larger *Ri*, see $Ri = 1.0$ in Fig. 10(c), the buoyancy effects on the local heat transfer rates, particularly that at the downstream part of the bottom wall, become more noticeable.

CONCLUDING REMARKS

Numerical solutions of mixed convection in a suddenly-expanded channel with a cold fluid injection

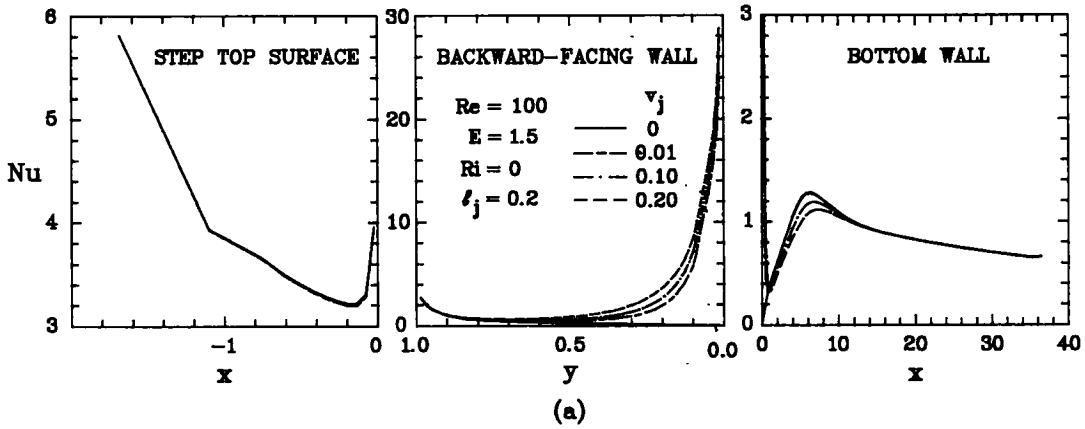

FIG. 10. Local heat transfer rates: (a) effects of cold fluid injection at (Re, E, l_j, Ri) = (100, 1.5, 0.2, 0); (b) buoyancy effects at (Re, E, v_j) = (100, 1.5, 0), and (c) buoyancy effects at (Re, E, v_j) = (50, 1.5, 0).

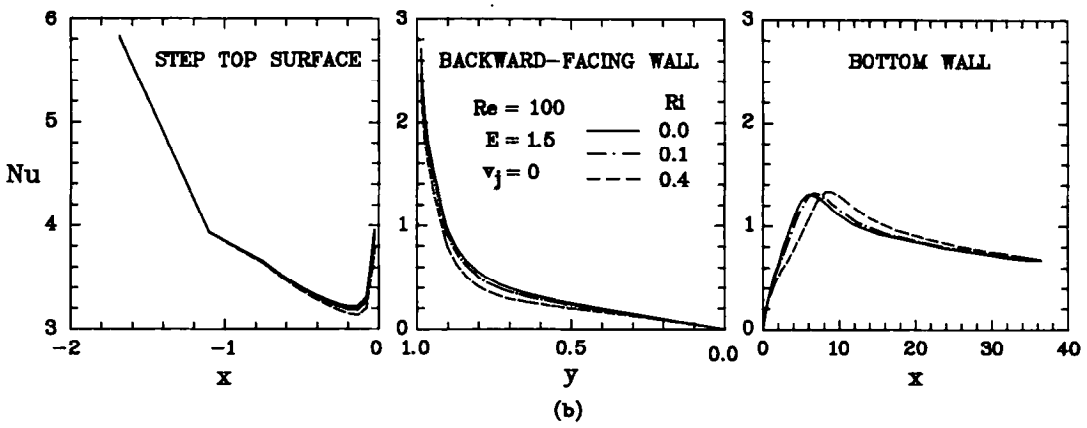

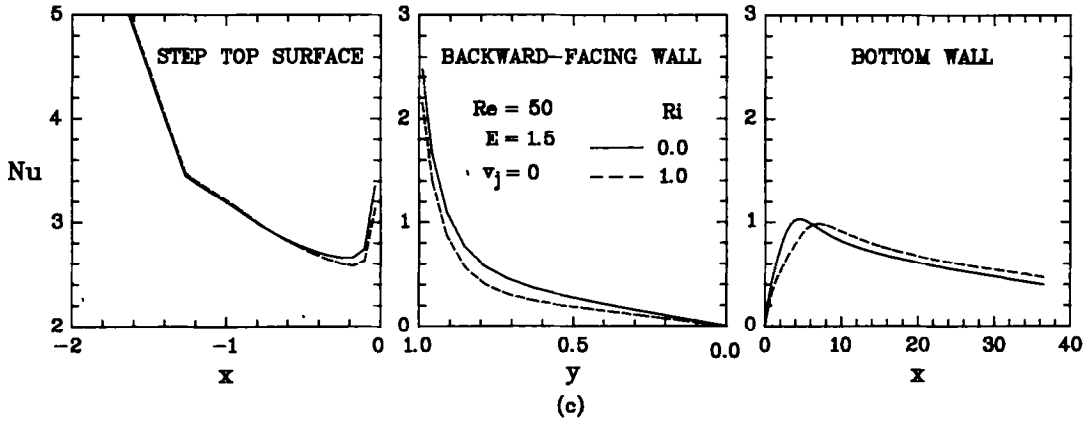

FIG. 10.—*Continued.*

has been developed. Based on the present results, the following conclusions can be drawn.

1. Both the effects of fluid injection and buoyancy enlarge the size of the recirculation zone behind the step. Bi-linear correlations are proposed for quick and accurate predictions of the reattachment length at various conditions of injection and buoyancy.

2. The cold fluid injection enhances the heat transfer on the backward-facing wall and slightly reduces that on the bottom wall. Globally, however, the injection has an advantageous effect on heat transfer. It is worth noting that a small amount of injection can provide a remarkable improvement in local heat transfer performance.

3. The buoyancy effect is beneficial to the heat transfer rate on the wall downstream of the separation bubble, but is disadvantageous to that in the recirculation zone.

REFERENCES

1. P. J. Roache and T. J. Mueller, Numerical solutions of laminar separated flows, *AIAA Jl* **8**, 530–538 (1970).
2. M. K. Denhan and M. A. Patrick, Laminar flow over a downstream facing step in a two dimensional channel, *Trans. Inst. Chem. Eng.* **52**, 361–367 (1974).
3. D. J. Aykins, S. J. Maskell and M. A. Patrick, Numerical predictions of separated flows, *Int. J. Numer. Methods Engng* **15**, 129–144 (1980).
4. C. E. Thomas, K. Morgan and C. Taylor, A finite element analysis of flow over a backward facing step, *Comput. Fluids* **9**, 265–278 (1981).
5. L. P. Hackman, G. D. Rauthby and A. B. Strong, Numerical prediction of flows over backward facing steps, *Int. J. Numer. Methods Fluids* **4**, 711–724 (1984).
6. B. F. Armaly, F. Durst and J. C. F. Pereira, Experimental and theoretical investigation of backward-facing step flow, *J. Fluid Mech.* **127**, 473–496 (1983).
7. J. A. Sethian and A. F. Ghonien, Validation study of vortex methods, *J. Comput. Phys.* **74**, 283–317 (1983).
8. S. Thangam and D. D. Knight, A computational scheme in generalized coordinates for viscous incompressible flows, *Comput. Fluids* **18**, 317–327 (1990).
9. E. J. Hall and R. H. Pletcher, Application of a viscous–inviscid interaction procedure to predict separated flows with heat transfer, *ASME J. Heat Transfer* **107**, 557–563 (1985).
10. E. M. Sparrow and W. Chuck, PC solutions for heat transfer and fluid flow downstream of an abrupt asymmetric enlargement in a channel, *Numerical Heat Transfer* **12**, 19–40 (1987).
11. S. F. Chou and J. S. Wu, The effect of natural convection generated from a horizontal blockage on horizontal channel flow. In *Transport Phenomena in Thermal Control* (Edited by G. J. Hwang), pp. 209–221. Hemisphere, New York (1989).

12. S. Habchi and S. Acharaya, Laminar mixed convection in a partially blocked, vertical channel, *Int. J. Heat Mass Transfer* **29,** 1711–1722 (1986).
13. J. T. Lin, B. F. Armaly and T. S. Chen, Mixed convection in buoyancy-assisting, vertical backward-facing step flows, *Int. J. Heat Mass Transfer* **33,** 2121–2132 (1990).
14. M. K. Chyu and S. G. Schwarz, Effects of bottom injection on heat transfer and fluid flow in rectangular cavities, *AIAA Jl. Thermophysics Heat Transfer* **4,** 521–526 (1990).
15. R. R. Chein and J. R. Jwo, Numerical study of laminar separated flow and heat transfer over rectangular heated block, *Proc. 7th Conf. CSME*, Hsinchu, Taiwan, ROC, 539–545 (1990).
16. S. V. Patankar, *Numerical Heat Transfer and Fluid Flow*. Hemisphere, Washington, D.C. (1981).